Received: 26 November 2020 | Revised: 24 February 2021 | Accepted: 25 February 2021

DOI: 10.1002/rcm.9074

PROTOCOL

Rapid Communications in Mass Spectrometry WILEY

Determination of magnesium isotopic ratios of biological reference materials via multi-collector inductively coupled plasma mass spectrometry

Samuel Le Goff[1] | Emmanuelle Albalat[1] | Anthony Dosseto[2] | Jean-Philippe Godin[3] | Vincent Balter[1]

[1]ENS de Lyon, Univ Lyon 1, Lyon, France

[2]Wollongong Isotope Geochronology Laboratory, School of Earth, Atmospheric and Life Sciences, University of Wollongong, Wollongong, NSW, Australia

[3]Nestlé Research, Institute of Food Safety and Analytical Sciences, Lausanne, Switzerland

Correspondence
S. Le Goff, ENS de Lyon, Univ Lyon 1, CNRS UMR 5276, LGL-TPE, F-69007, Lyon, France.
Email: samuel.le-goff@ens-lyon.fr

Funding information
Société des Produits Nestlé SA (Lausanne, Switzerland)

Rationale: Despite a wide range of potential applications, magnesium (Mg) isotope composition has been so far sparsely measured in reference materials with a biological matrix, which is important for the quality control of the results. We describe a method enabling the chemical separation of Mg in geological and biological materials and the determination of its stable isotope composition.

Methods: Different geological (BHVO-1, BHVO-2, BCR-1, and IAPSO) and biological (SRM-1577c, BCR-383, BCR380R, ERM-CE464, DORM-2, DORM-4, TORT-3, and FBS) reference materials were used to test the performance of a new sample preparation procedure for Mg isotopic analysis. The procedure consisted of a simple three-stage elution method to separate Mg from the matrix. Mg isotopic analyses were performed in two different laboratories and with three different multi-collector inductively coupled plasma mass spectrometry instruments.

Results: The biological reference materials show a wide range of δ^{26}Mg values (relative to DSM3 standard), spanning over 2‰, from 0.52 ± 0.29‰ (2SD, n = 7) in bovine liver (SRM-1577c) to −1.45 ± 0.20‰ (2SD, n = 5) in tuna fish (ERM-CE464), with an external precision of 0.03‰ (2SD, n = 85).

Conclusions: This study indicates that isotopic measurements of Mg in biological reference materials show good performance, with the results being within the accepted range. We confirmed that δ^{26}Mg values in liver are the most positive of all biological materials reported so far.

1 | INTRODUCTION

Magnesium (Mg) has three stable isotopes, ^{24}Mg, ^{25}Mg, and ^{26}Mg, with relative abundances of 78.99%, 10.00%, and 11.01%. Interest in the Mg isotopic systematics for biological systems arose from the discovery that the Mg isotope composition of chlorophyll-a extracted from experimentally grown cyanobacteria is depleted in heavy isotopes relative to the culture media by about 1‰.[1] Further studies experimentally scrutinized the mechanisms responsible for the chlorophyll-related Mg isotope fractionation in both unicellular organisms[2,3] and higher plants.[4–6] The first investigation of the Mg isotope systematics in animals focused on the potential of using the enamel Mg isotope composition to reconstruct past trophic chains.[7,8] A basic scheme of the Mg isotope fractionation in the body was then proposed to explain the observed increase in the δ^{26}Mg value up the trophic chain.[8] Recently, it has been discovered that the serum δ^{26}Mg value in patients with type 1 diabetes is significantly lower than in healthy controls, suggesting that Mg isotope changes might be a biomarker of metabolic deregulations.[9] However, Mg isotopic compositions have rarely been reported for biological reference materials,[9–13] thus limiting quality control assessment for biological samples.

The aim of this work was to measure the Mg isotope composition by multi-collector inductively coupled plasma-mass spectrometry (MC-ICP-MS) in a series of certified reference materials with a large diversity of organic matrices, that is, SRM-1577c (bovine liver), BCR-383 (green beans), BCR-380R (whole milk), ERM-CE464 (tuna fish), DORM-2 and DORM-4 (fish protein), TORT-3 (lobster hepatopancreas), and fetal bovine serum (FBS). To measure these samples, we developed a new three-stage elution method to separate Mg from the other elements. The efficiency of the elution method was monitored by measuring the δ^{26}Mg value of the well-described BHVO-1, BHVO-2, and BCR-1 basalts and IAPSO seawater international reference materials. Finally, to assess the robustness of the overall method, the Mg isotope compositions were measured in two different laboratories with three different MC-ICPMS instruments.

2 | MATERIALS AND METHODS

2.1 | Materials and reagents

The reference material digestion and Mg extraction steps were all carried out in a clean laboratory in laminar flow hoods. Acids (HNO_3 and HCl) were double-distilled to reduce blank contaminations. Suprapur 30% H_2O_2 (Fisher Chemical, Hampton, NH, USA) was used. Ultrapure water (resistivity > 18.2 MΩ·cm) was obtained from a Milli-Q Element water purification system (Merck Millipore, Bedford, MA, USA). Polypropylene chromatographic columns (Bio-Rad, Temse, Belgium) filled with 2 mL of Bio-Rad AG1-X8 resin, chloride form 100-200 mesh size, were used for the first stage of chromatography. Quartz chromatographic columns (custom-made) filled with 2 mL of Bio-Rad AG50W-X12 resin, hydrogen form 200-400 mesh size, were used for the second stage of chromatography. Finally, Teflon© columns (custom-made using retractable Teflon) filled with 210 μL of Bio-Rad AG50W-X12 resin, hydrogen form 200-400 mesh size, were used for the third stage of chromatography. We used BHVO-1 (USGS, Reston, VA, USA), BHVO-2 (USGS), and BCR-1 (USGS) basalts for geological reference materials, the IAPSO (OSIL) certified reference seawater standard, and SRM-1577c (bovine liver), BCR-383 (green beans), BCR-380R (whole milk), ERM-CE464 (tuna fish), DORM-2 and DORM-4 (fish protein), TORT-3 (lobster hepatopancreas), and FBS as biological reference materials. The characteristics of all the reference materials are summarized in Table S1 (supporting information).

2.2 | Sample digestion

Materials of biological origin require aggressive treatment to eliminate the organic matter before chromatographic purification. Reference materials with an organic matrix were pre-digested using 10 mL of 15 M distilled HNO_3 at room temperature in clean Teflon beakers (Savillex™, Eden Prairie, MN, USA). Then 3 mL of Suprapur 30% H_2O_2 was added, and the resulting mixture was heated at 150°C for more than 12 h, regularly degassed, and finally evaporated to dryness. Organic samples were also digested in clean PTFE microwave bombs using 4 mL of 15 M distilled HNO_3 and 1 mL of Suprapur 30% H_2O_2. The bombs were then sealed and placed in a Milestone Ethos microwave (Milestone, Sorisole, Italy) set to ramp up to 180°C in 20 min and remain at 180°C for 40 min. The solutions were then evaporated to dryness on a hot plate at 90°C in Teflon© beakers.

Rock reference materials (BHVO-1, BHVO-2, and BCR-1 from USGS) were digested with a mixture of 5 mL of 27 M distilled HF and 2.5 mL of 15 M distilled HNO_3 at 120°C for 12 h and evaporated to dryness. Fluorides were further dissolved using 2 mL of 6 M HCl, heated on a hotplate at 100°C for 12 h, and then evaporated to dryness.

2.3 | Purification of Mg using ion exchange chromatography

To avoid any isotopic bias, it is crucial to ensure that the sample preparation method can selectively isolate Mg from the other elements present in the samples. A protocol using ion exchange chromatography in three stages with three different columns was optimized (Table 1). The first column is a polypropylene chromatographic column filled with 2 mL of AG1-X8 resin, chloride form 100-200 mesh size. The resin was cleaned with 6 M HCl and 0.5 M HNO_3 and then conditioned with 6 M HCl. This first stage removed Fe, which is not an interfering element but must be

TABLE 1 Ion exchange protocols for the chromatographic separation of Mg

Step	Eluent	Vol. (mL)
1. Fe elimination		
AG1-X8 (100-200 mesh)-2 mL (Bio-Rad Poly-Prep® chromatography columns 2 mL ø0.8 mm)		
Condition	6 N HCl	10
Load	6 N HCl	0.5
Elution (Mg)	6 N HCl	0.5 + 8.5
Washout (Fe, Zn)	0.5 N HNO_3	10
2. Matrix elimination		
AG50W-X12 (200-400 mesh)-2 mL ø0.76 mm		
Condition	1 N HCl	10
Load	1 N HCl	0.5
Elution (matrix)	1 N HCl	0.5 + 17
Elution (Mg)	1 N HCl	18-42.5
Washout (Ca, Sr)	6 N HCl	10
3. Matrix elimination		
AG50W-X12 (200-400 mesh)-210 μL ø0.42 mm		
Condition	0.4 N HCl	2.5
Load	0.4 N HCl	0.3
Elution (matrix)	0.4 N HCl	0.7 + 12
Elution (Mg)	1 N HCl	3.5
Cleaning	6 N HCl	2.5

eliminated to avoid any matrix effects. This was achieved by eluting most of the elements (Ca, Mg, P, S, K, Mn, and Na), using 10 mL of 6 M HCl, except for Cu, Fe, and Zn which were eluted with 10 mL of 0.5 M HNO_3. The second column is a quartz chromatographic column filled with 2 mL of AG50W-X12 resin, hydrogen form 200-400 mesh size. The resin was cleaned with 6 M HCl and then conditioned with 1 M HCl. The aim of the second stage was to remove the matrix (S, P, Na, and Ca), and this was performed by collecting the 18-42 mL (i.e., 24 mL) fraction of 1 M HCl passed through a custom-made quartz column filled with 2 mL AG50W-X12 resin. The third column is a Teflon© column filled with 210 μL of AG50W-X12 resin, hydrogen form 200-400 mesh size. The resin was cleaned with 6 M HCl and then conditioned with 0.4 M HCl. The aim of the third stage was to dispose of the remaining elements, essentially K. The procedure used was similar to that in the second stage, but the elution volume was reduced by eluting Mg (and Mn) with 3.5 mL of 1 M HCl after passing 13 mL of 0.4 M HCl through the custom-made Teflon column. This last stage was carried out twice (optional fourth step) for samples with a high Mg/K ratio. Finally, the Mg fraction was redissolved using 3 mL of concentrated HNO_3 to remove any remaining organics and then evaporated to dryness.

2.4 | Isotopic analysis

The use of MC-ICP-MS requires an efficient separation of Mg from samples because of potential isobaric interferences[14] and matrix effects, that is, polyatomic species (C_2^+, $C_2H_2^+$, C_2H^+, CN^+, and NaH^+) and doubly charged ions ($^{48}Ca^{2+}$, $^{48}Ti^{2+}$, $^{50}Ti^{2+}$, $^{50}V^{2+}$, $^{50}Cr^{2+}$, and $^{52}Cr^{2+}$). The present study describes a method that both reduces and corrects for these potential polyatomic and divalent interferences on the ^{24}Mg, ^{25}Mg, and ^{26}Mg isotopes. The Mg isotopic composition of the samples was measured at the Laboratoire de Géologie de Lyon (LGL, Ecole Normale Supérieure de Lyon, France) using either a Thermo Scientific™ Neptune Plus™ MC-ICP-MS instrument (Thermo Fisher Scientific, Bremen, Germany) or a Nu Plasma 1700 MC-ICP-MS instrument (Nu Instruments Ltd™, Wrexham, UK). The Mg isotopic composition was also measured at the Wollongong Isotope Geochronology Laboratory (WIGL, University of Wollongong, Australia) using a Neptune Plus™ MC-ICP-MS instrument. Standard and sample Mg solutions were prepared at 0.5 mg/L in 0.05 M HNO_3 yielding typical signal intensities of 30 V, 4 V, and 5 V for ^{24}Mg, ^{25}Mg, and ^{26}Mg, respectively, on both Neptune Plus instruments, and 12 V, 1.5 V, and 2 V for ^{24}Mg, ^{25}Mg, and ^{26}Mg, respectively, on the Nu Plasma 1700. Solutions were introduced into the plasma using a 100 μL/min glass concentric nebulizer mounted onto a double spray chamber with cyclonic and Scott-type sub-units on the Neptune Plus and a cyclonic spray chamber on the Nu Plasma 1700. Mg isotope ratio measurements were performed at low mass resolution on the middle of the peak, using three Faradays collectors (L3, C, and H3) connected to $10^{11}\Omega$ resistors on both Neptune Plus MC-ICP-MS instruments, and at low mass resolution on the middle of the peak, using three Faradays collector (L5, Ax, and H6) connected to $10^{11}\Omega$ resistors on the Nu plasma 1700. The instrument's settings are summarized in Table 2. Acid and total procedure blanks were measured at the beginning of each analytical sequence to evaluate their contribution to the total Mg signal intensity. The acid blank contribution was found to be systematically negligible, regardless of the analytical conditions. The total procedure blank ^{24}Mg signal was typically measured at 4.2×10^{-3} V on the Neptune Plus, thus representing a 0.01% contribution to an overall Mg signal at 0.5 mg/L. Two Mg isotope reference solutions, UKAS (in-house standard) and Cambridge-1,[15] were measured regularly as external standards to check the accuracy and the reproducibility of the measurements. The reference material DSM3 (provided by Dead Sea Magnesium Ltd, Beer Sheva, Israel) was used during isotopic analysis for a standard-sample bracketing approach. External correction in a sample-standard bracketing approach was applied for instrumental mass bias correction. The $^{26}Mg/^{24}Mg$ ratio is expressed in delta notation relative to the DSM3 reference material and calculated as follows:

$$\delta^{26}Mg = \left[\frac{(^{26}Mg/^{24}Mg)_{Sample}}{(^{26}Mg/^{24}Mg)_{DSM3}} - 1\right].$$

Some troublesome elements of the biological matrix may remain in the final solution after the ion exchange chromatography and potentially affect the accuracy and precision of Mg isotope analysis. In this study, we examined the effect of Na, Li, Fe, Ca, Mn, and K by doping the UKAS solution with varying amounts of these metals to evaluate the potential offset on the $\delta^{26}Mg$ value.

3 | RESULTS

3.1 | Sample preparation for Mg isotopic measurements

We first evaluated the quality of the dissolution method by comparing the results of element concentration (Ca, Cu, Fe, K, Mg, Mn, P, S, and Zn) in all the reference materials (SRM-1577c, BCR-383, BCR-380R, ERM-CE464, DORM-2, DORM-4, TORT-3, and FBS), with those published in Sauzéat et al.[16] Our data strongly correlate with certified values (R = 0.99; P-value $<2.2 \times 10^{-16}$; n = 37) according to a linear regression with a slope of 0.96 (±0.01) and an offset at origin of −163 (±742), showing that the dissolution step was efficient at solubilizing all the elements. We also calculated the yields of Mg for the whole elution method and found quantitative yields (from 80% to 106%) for all the reference materials (SRM-1577c, BCR-383, BCR-380R, ERM-CE464, DORM-2, DORM-4, and TORT-3), except for FBS (where the Mg yield was 77%). All the concentration results and yield values are reported in Table S2 (supporting information).

Elution profiles are presented in Figure 1 for the bovine liver reference material SRM-1577c. Iron was efficiently removed in the first steps along with Cu and Zn by collecting the first 9.5 mL of 6 N HCl. The resin was cleaned from Fe, Cu, and Zn with 10 mL of 0.5 N HNO_3 (Figure 1A). The second and third elutions on cationic resin were aimed at discarding specific metals (Na, K, P, S, and Ca) from the

TABLE 2 Instrument settings and data acquisition parameters for multi-collector inductively coupled plasma-mass spectrometry (MC-ICP-MS) analysis

Lab	LGL		WIGL
MC-ICP-MS instrument	Thermo Scientific® Neptune® Plus	NuPlasma 1700 HR-MC-ICPMS	Thermo Scientific® Neptune® Plus
RF power	1200 W	1350 W	1200 W
Cooling gas flow rate	16 L/min Ar	≈ 14 L/min Ar	16 L/min Ar
Auxiliary gas flow rate	≈ 0.80 L/min Ar	≈ 1.23 L/minAr	≈ 0.80 L/min Ar
Sample gas flow rate	≈ 1.10 L/min Ar	≈ 42.7 psi Ar	≈ 1.12 L/min Ar
Sampler cone	Standard-cone (Ni)	Wet plasma 1.15 mm orifice, 319-645	Standard-cone (Ni)
Skimmer cone	X-cone (Ni)	Wet plasma 0.6 mm orifice, WA6, 319-497	X-cone (Ni)
Nebulizer	Glass nebulizer micromist	Glass nebulizer micromist	PFA nebulizer
Sample uptake rate	100 μL/min	100 μL/min	100 μL/min
Spray chamber	Double spray chamber with cyclonic and Scott-type sub-units	Cyclonic spray chamber	Double spray chamber with cyclonic and Scott-type sub-units
Data acquisition parameters			
Detection system	Faraday cups	Faraday cups	Faraday cups
Cup configuration	24 Mg (L3), 25 Mg (C), 26 Mg (H3)	24 Mg (L5), 25 Mg (Ax), 26 Mg (H6)	24 Mg (L3), 25 Mg (C), 26 Mg (H3)
Resolution mode	Low	Low	Low
Signal analysis protocol	4.194 s integration per cycle, 40 cycles	10.0 s integration per cycle, 40 cycles	4.194 s integration per cycle, 40 cycles
Wash-out time	180 s (0.5 M HNO_3) + 180 s (0.05 M HNO_3)	180 s (0.5 M HNO_3) + 180 s (0.05 M HNO_3)	180 s (0.5 M HNO_3) + 180 s (0.05 M HNO_3)

biological sample matrices, but others like K and Mg cannot be separated in 1 N HCl (Figure 1B). This also holds for Mn, which is a minor element in biological samples. A third stage was thus necessary to isolate Mg from K, which was achieved on the third column by passing 13 mL of 0.4 N HCl (Figure 1C). Finally, Mg was eluted with 3.5 mL of 1 N HCl although it cannot totally be separated from Mn. The third elution stage is repeated for samples with an initial high K/Mg ratio (>10^{-2}). The elution method was also tested on pure Mg reference standard solutions, that is, the Cambridge-1, DSM3, and an in-house standard (UKAS), which gave Mg isotope compositions that were undistinguishable from measurements of raw solutions.

Blanks of the whole procedure did not exceed 11 ng of Mg (n = 6). This is about 2500 times smaller than the Mg amount extracted from the samples analyzed in this study (about 30 μg of Mg) and therefore could not affect the accuracy of the measured Mg isotopic composition.

3.2 | Mass-dependent fractionation of Mg composition

All the measured isotopic compositions of biological samples and standards are summarized in Table S3 (supporting information). The quality of the isotopic results was assessed by the calculation of the exponent β relating the mass-dependent fractionation factors for two isotope ratios, which is different for kinetically and thermodynamically controlled fractionation.[17] A plot of δ^{26}Mg vs δ^{25}Mg (Figure 2) yields the mass fractionation relationship in three-isotope spaces, allowing us to calculate the β value, which corresponds to the slope of the best-fit linear regression. We obtained a β value of 0.517, which is in good agreement with the value of the terrestrial line,[15] and between the theoretical kinetically controlled (0.511) and thermodynamically controlled (0.521) β values.[17]

3.3 | Analytical precision of Mg isotopic measurements

The quality of the isotopic results can also be assessed by evaluating the long-term reproducibility of the results for external standards, namely UKAS and Cambridge-1 (Figure 3). Over more than 1 year of measurements, the average δ^{26}Mg value of Cambridge-1 was found to be −2.60 ± 0.03‰ (n = 85, 2SD), in agreement with a reference value of −2.58 ± 0.14‰ (n = 35, 2SD).[15] Over this timespan, the in-house UKAS standard solution provided an average δ^{26}Mg value of −0.60 ± 0.03‰ (n = 46, 2SD, Figure 3).

3.4 | Influence of matrix effects on Mg isotopic measurements

The effect of matrix impurities on the δ^{26}Mg value was simulated by doping the UKAS solution with known amount of K, Na, Ca, and Fe. The elements considered are those potentially abundant in

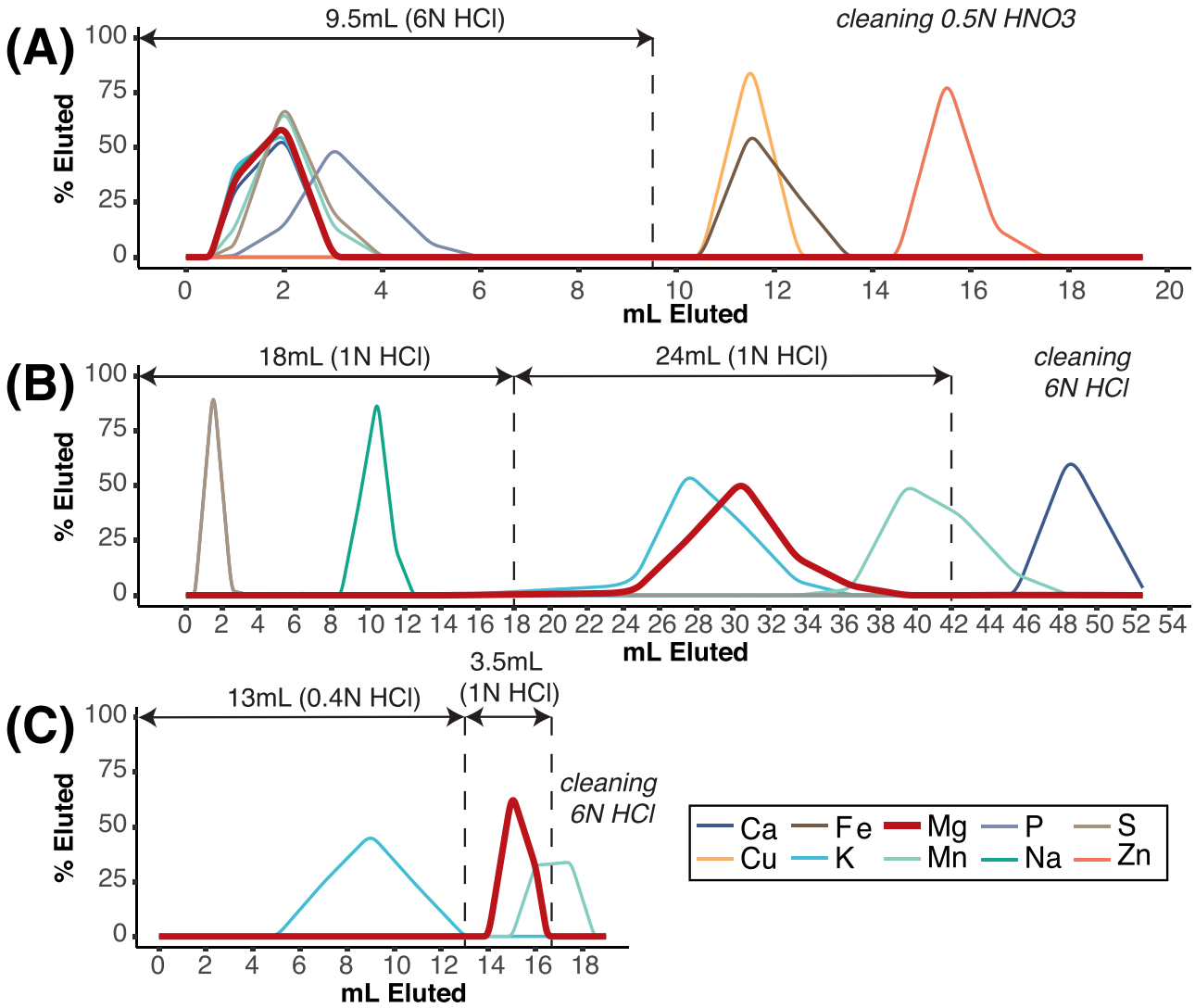

FIGURE 1 Elution profiles of selected elements on A, AG1-X8, B, AG50W-X12, and C, AG50W-X12 for SRM-1577c (bovine liver). Each curve represents the mass percentage of the eluted element as a function of the volume of eluting solution

biological matrices, plus Mn and Li, which are minor elements but are hardly separated from Mg in cationic resins in the case of Mn (Figure 1[18]). The results are illustrated in Figure 4 and show that the accuracy of the δ^{26}Mg value is not affected either by the presence of K even with a K/Mg ratio up to 5 (Figure 4A)—the K/Mg ratio in biological samples is about 14—or by the presence of Fe and Mn—even with a high Mg-normalized ratio of 2 (Figure 4B and C). Note that the Fe/Mg and Mn/Mg ratios are usually lower than 10^{-1} and 10^{-2}, respectively, in biological samples. However, an important scattering of the δ^{26}Mg value was observed when Na or Ca was added to the UKAS solution, even with a low Mg-normalized ratio of 0.02 (Figure 4D and E). Attention must be paid to these elements as the Na/Mg and Ca/Mg ratios can be >10 in some biological matrices (Table S3, supporting information). The highest reaction of the δ^{26}Mg value to the doping of the UKAS solution was obtained with Li, which shifted the δ^{26}Mg value by about +0.1‰ with a Li/Mg ratio of 0.05 and to −0.3‰ with a Li/Mg ratio of 0.5 (Figure 4F). We did not monitor Li during the elution profiles; however, Li is in very low concentration in biological samples (5-1000 ppb) and is therefore not expected to interfere with Mg isotope analysis.

3.5 | Mg isotope composition in geological and biological reference materials

Until very recently,[9,11–13] Mg isotope compositions were not measured in certified reference materials of biological origin. In view of the development of isotopic analysis in biological materials, it was thus necessary to also validate our new analytical method for determining isotopic ratios of Mg after chromatographic extraction of geological reference materials with known δ^{26}Mg values. To this end, we measured the δ^{26}Mg value of the BHVO-1, BHVO-2, and BCR-1 basalt standards and the IAPSO seawater standard (Table S3, supporting information).

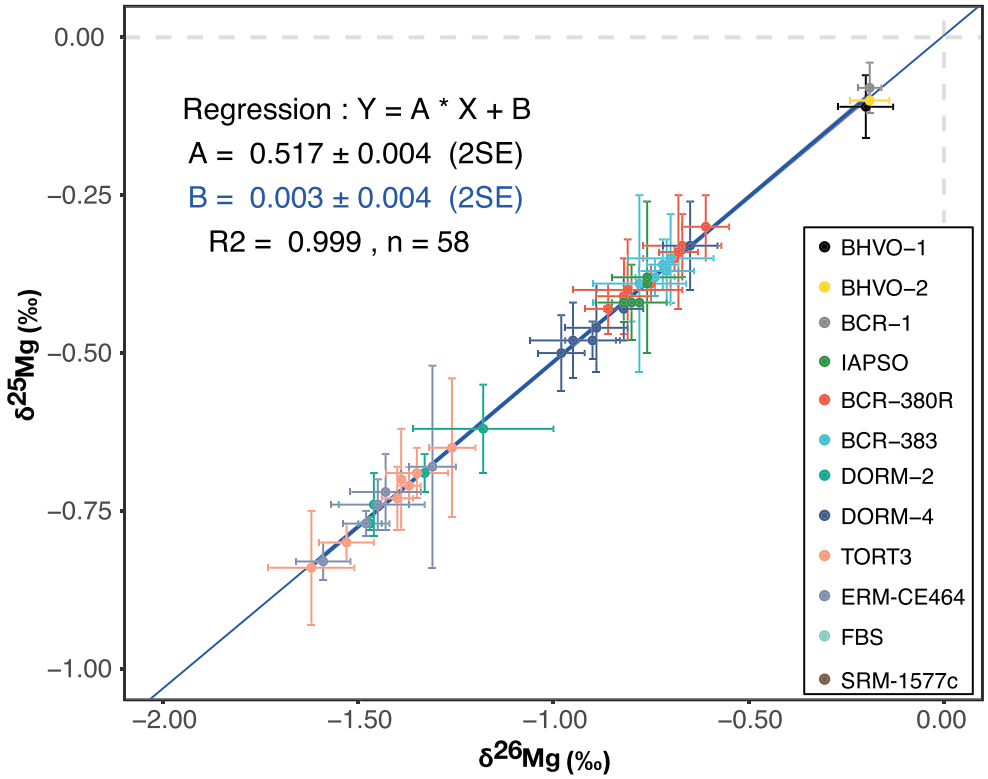

FIGURE 2 Mass fractionation in three-isotope space ($\delta^{25/24}$Mg versus $\delta^{26/24}$Mg) for the reference materials analyzed in this study. Error bars represent two standard deviations of the mean

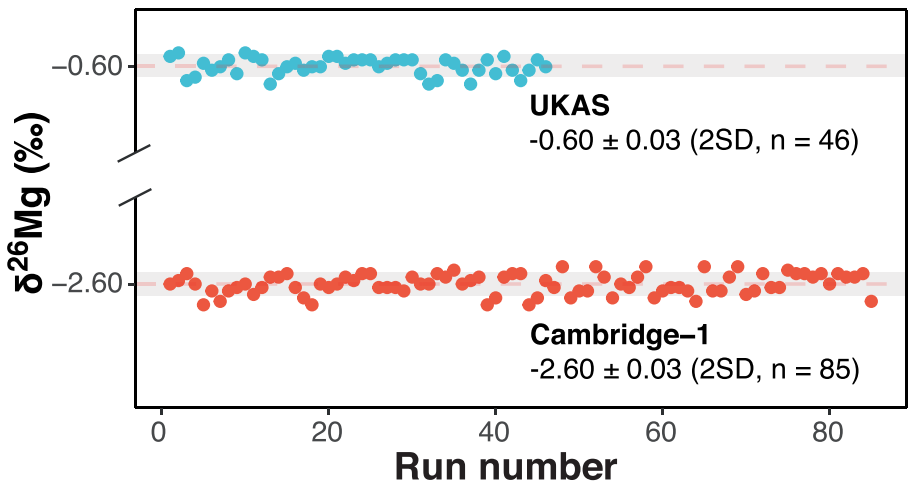

FIGURE 3 Long-term reproducibility of δ^{26}Mg measurement for Mg solutions Cambridge-1 and UKAS, in-house standard. The long-term external precision was better than ±0.03‰ (±2SD)

We obtained an average δ^{26}Mg value of −0.20 ± 0.07‰ (2SD, n = 6), −0.19 ± 0.05‰ (2SD, n = 2), −0.19 ± 0.03‰ (2SD, n = 2), and −0.78 ± 0.07‰ (2SD, n = 12) for BHVO-1, BHVO-2, BCR-1, and IAPSO, respectively (Figure 5). These values are in very good agreement with published data (Figure 5) and suggest that our chromatographic extraction of Mg is efficient for different matrices, whether geological or biological. We then measured the δ^{26}Mg value (ranging from −1.45 ± 0.20‰ to 0.52 ± 0.29‰) in 50 independent aliquots of eight biological reference materials (Figure 6; Table S3, supporting information).

4 | DISCUSSION

The sample preparation takes advantages of two previous studies[19,20] for the first and second steps of elution, and is based on K having a lower partitioning coefficient than Mg in dilute HCl solution in cationic resins[21] for the third step of elution. Our elution protocol offers several advantages over currently available methods. Grigoryan et al[11] proposed a one-stage only elution protocol in cationic resin using dilute HCl and acetone. However, in this protocol a significant tailing effect of the Mg elution curve was observed, such that Mg was collected throughout 20 mL. Another disadvantage was the presence

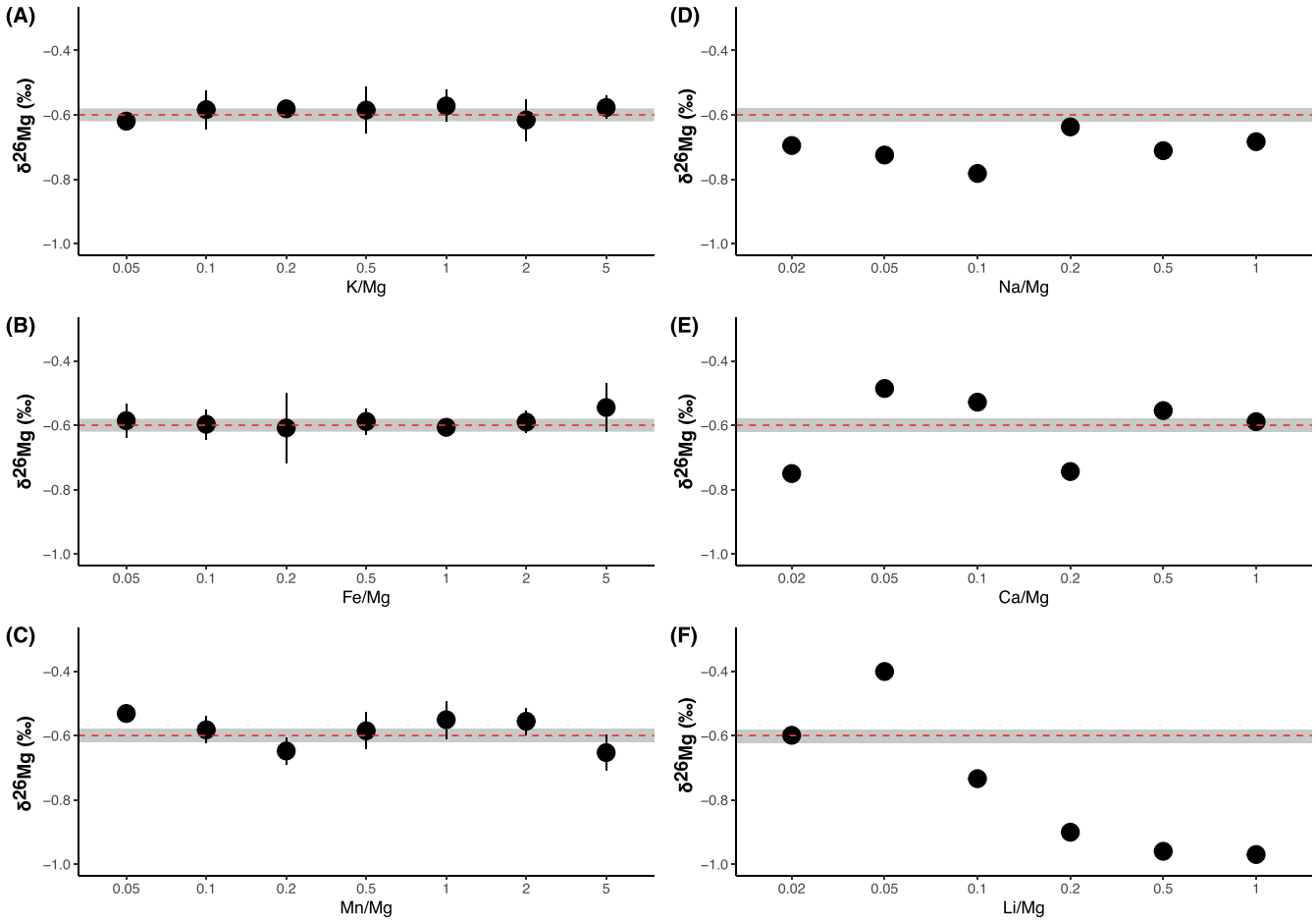

FIGURE 4 Matrix effects of some elements on the UKAS Mg isotopic ratio. The dotted red line indicates the average δ^{26}Mg value for the in-house UKAS standard, and the shaded area is for two standard deviations of the mean

of acetone in this protocol, which is a source of carbon that produces polyatomic ions (C_2^+, C_2H^+, $C_2H_2^+$, and CN^+) interfering with all Mg isotopes. In another recent study, Bao et al[13] used a three-stage elution protocol in addition to a precipitation step. Our protocol is also based on a three-stage method. Although it could be reduced to two stages only, assuming that Fe is of little influence on the accuracy of the Mg isotope composition (confirmed by our matrix doping experiments, Figure 4B), the three-stage approach was applied to all samples.

The 2SD values obtained in the present study for rock and seawater reference materials range from 0.02 to 0.09‰, with an average value of ±0.05‰ (n = 8, Table S3, supporting information). These numbers are slightly better than those published in the literature, for which the 2SD values range from 0.01[22,23] to 0.19‰,[24,25] with an average value of ±0.10‰ (n = 83). For biological reference materials, the 2SD range in the present study is from 0.08 to 0.29‰, with an average value of ±0.19‰ (n = 49, Table S3, supporting information). Other studies also show a greater variability of external reproducibility in materials of biological origin than in inorganic materials.[9,11–13] It is possible that significant amounts of complex residual organics remain after the aggressive acid and H_2O_2 mineralization, leading to a more unstable behavior of the matrix during chromatographic separation (Table S1, supporting information).

Taken together, these comparisons suggest that the overall method proposed in the present study yields reproducible Mg isotope compositions, in both inorganic and organic matrices. The results must be challenged in further studies to validate their accuracy.

To complement this work, isotope measurements of Mg from two reference materials (BCR-383 and TORT-3) were also performed on two other MC-ICP-MS instruments (Table 2). The Nu Plasma 1700 instrument gave identical δ^{26}Mg values (BCR-383: δ^{26}Mg = −0.78 ± 0.12‰, n = 4; TORT-3: δ^{26}Mg = −1.26‰, n = 1) to the Lyon Neptune™ instrument (BCR-383: δ^{26}Mg = −0.73 ± 0.09‰, n = 4; TORT-3: δ^{26}Mg = −1.43 ± 0.25‰, n = 6) (Table S3, supporting information). Finally, comparisons of inter-laboratories (LGL and WIGL) were carried out on the Neptune™ instruments (with similar instrument settings), which also produced identical results (Figure 6; Table S3, supporting information).

The δ^{26}Mg values of biological reference materials cover a wide range, spanning over 2‰ from to −1.45 ± 0.20‰ (n = 5, 2SD) in tuna fish (ERM-CE464) to 0.52 ± 0.29‰ (n = 7, 2SD) in bovine liver SRM-1577c. Marine materials, that is, tuna fish (ERM-CE464) and lobster

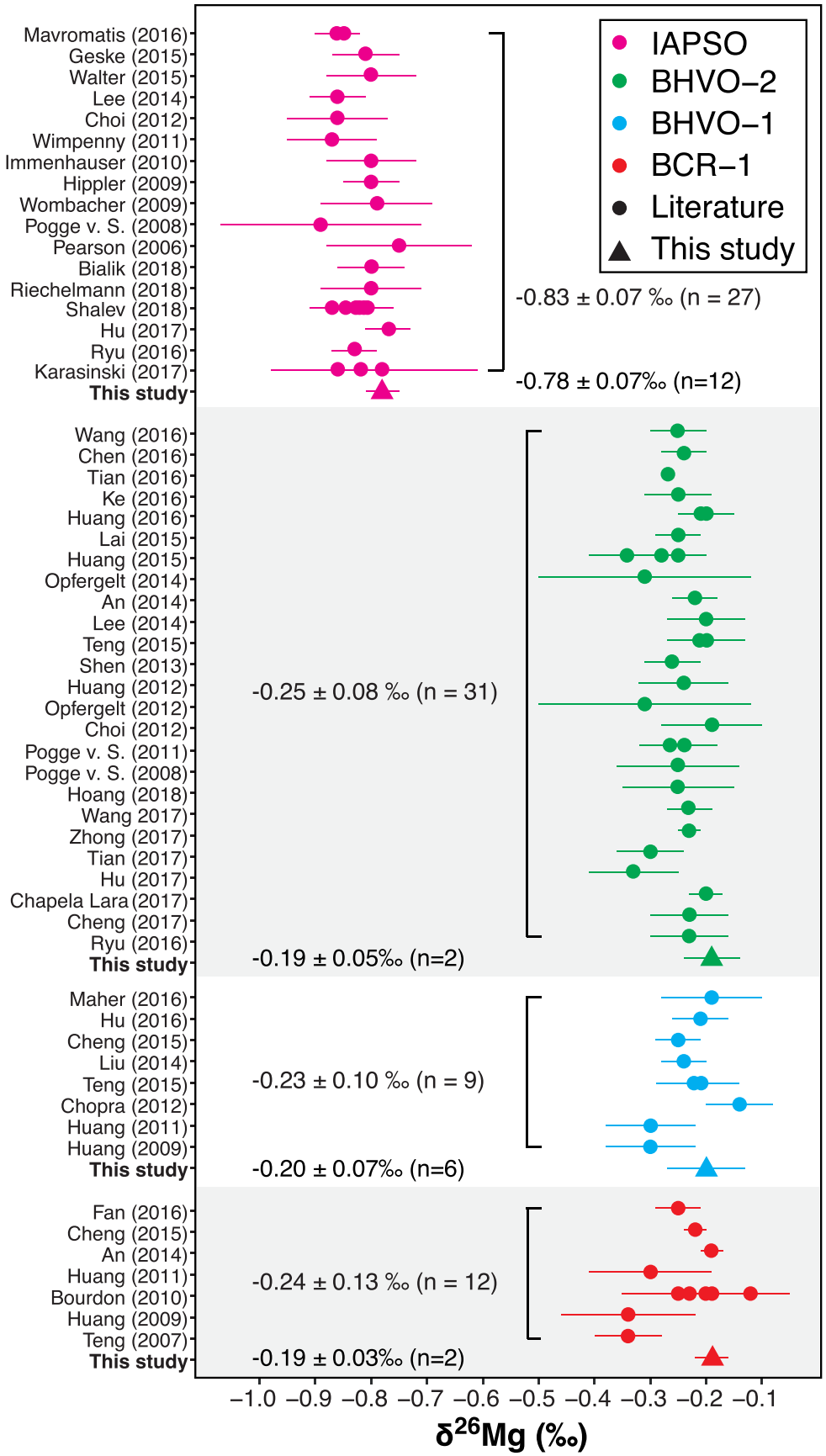

FIGURE 5 Distribution of δ^{26}Mg values for rock and seawater reference materials found in the literature along with the results of the present study. Error bars represent two standard deviations of the mean

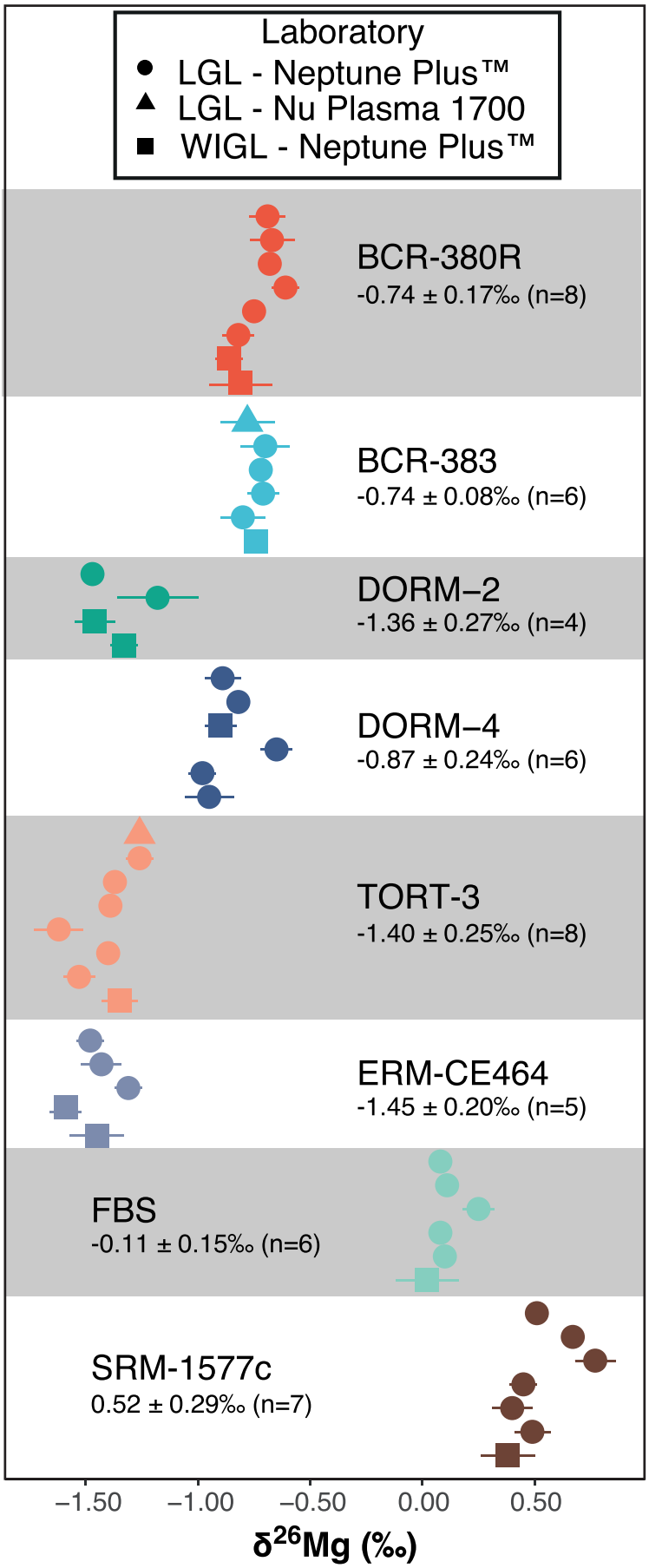

FIGURE 6 Distribution of δ^{26}Mg values for biological reference materials measured in the present study. Each point is a sample aliquot that has completed the entire protocol. Error bars represent two standard deviations of the mean

hepatopancreas (TORT-3) exhibit the most ^{26}Mg-depleted isotopic ratios. DORM-2 and DORM-4 are two fish protein homogenates, but it is not specified whether they were prepared from freshwater or seawater fish. The liver is the biological material the most enriched in heavy Mg isotope within all published biological δ^{26}Mg values.[11,12] The old and now-exhausted SRM1577a reference material yielded a δ^{26}Mg value of 0.34 ± 0.03‰, 2SD, n = 2), thus also enriched in the heavy Mg isotope.[11,12] This highlights the involvement of Mg in hepatic metabolic processes and the potential sensitivity of the Mg isotope composition to hepatic pathological conditions.[26,27]

5 | CONCLUSION

This study validates a protocol for the elution of Mg for the subsequent measurement of stable isotope compositions which is suited for various types of biological materials in the context of bio-medical studies, or by extension for environmental studies. This procedure efficiently eliminates any interfering elements potentially present in the biological and geological matrices, beyond the required levels for accurate isotopic measurement and without chromatographically induced fractionation or contamination.

ACKNOWLEDGMENTS

The authors thank an associate editor, four anonymous reviewers, and P. Louvat for their thorough and insightful comments on an earlier version of this manuscript. The authors also thank Société des Produits Nestlé SA (Lausanne, Switzerland) for funding this study.

PEER REVIEW

The peer review history for this article is available at https://publons.com/publon/10.1002/rcm.9074.

ORCID

Samuel Le Goff https://orcid.org/0000-0001-7090-6914
Vincent Balter https://orcid.org/0000-0002-9236-4834

REFERENCES

1. Black JR, Yin Q, Casey WH. An experimental study of magnesium-isotope fractionation in chlorophyll-a photosynthesis. *Geochim Cosmochim Acta*. 2006;70(16):4072-4079. https://doi.org/10.1016/j.gca.2006.06.010
2. Pokharel R, Gerrits R, Schuessler JA, et al. Magnesium stable isotope fractionation on a cellular level explored by cyanobacteria and Black fungi with implications for higher plants. *Environ Sci Technol*. 2018;52(21):12216-12224. https://doi.org/10.1021/acs.est.8b02238
3. Isaji Y, Yoshimura T, Araoka D, et al. Magnesium isotope fractionation during synthesis of chlorophyll a and bacteriochlorophyll a of benthic phototrophs in hypersaline environments. *ACS Earth Space Chem*. 2019;3(6):1073-1079. https://doi.org/10.1021/acsearthspacechem.9b00013
4. Bolou-Bi EB, Poszwa A, Leyval C, Vigier N. Experimental determination of magnesium isotope fractionation during higher plant growth. *Geochim Cosmochim Acta*. 2010;74(9):2523-2537. https://doi.org/10.1016/j.gca.2010.02.010
5. Wang Y, Wu B, Berns AE, Xing Y, Kuhn AJ, Amelung W. Magnesium isotope fractionation reflects plant response to magnesium deficiency in magnesium uptake and allocation: A greenhouse study with wheat. *Plant and Soil*. 2020;455(1–2):93-105. https://doi.org/10.1007/s11104-020-04604-2
6. Moynier F, Fujii T. Theoretical isotopic fractionation of magnesium between chlorophylls. *Sci Rep*. 2017;7(1):6973. https://doi.org/10.1038/s41598-017-07305-6
7. Martin JE, Vance D, Balter V. Natural variation of magnesium isotopes in mammal bones and teeth from two south African trophic chains. *Geochim Cosmochim Acta*. 2014;130:12-20. https://doi.org/10.1016/j.gca.2013.12.029
8. Martin JE, Vance D, Balter V. Magnesium stable isotope ecology using mammal tooth enamel. *Proc Natl Acad Sci*. 2015;112(2):430-435. https://doi.org/10.1073/pnas.1417792112
9. Grigoryan R, Costas-Rodríguez M, Van Laecke S, Speeckaert M, Lapauw B, Vanhaecke F. Multi-collector ICP-mass spectrometry reveals changes in the serum mg isotopic composition in diabetes type I patients. *J Anal at Spectrom*. 2019;34(7):1514-1521. https://doi.org/10.1039/C9JA00097F
10. Bolou-Bi EB, Vigier N, Brenot A, Poszwa A. Magnesium isotope compositions of natural reference materials. *Geostand Geoanal Res*. 2009;33(1):95-109. https://doi.org/10.1111/j.1751-908X.2009.00884.x
11. Grigoryan R, Costas-Rodríguez M, Vandenbroucke RE, Vanhaecke F. High-precision isotopic analysis of mg and ca in biological samples using multi-collector ICP-mass spectrometry after their sequential chromatographic isolation – Application to the characterization of the body distribution of mg and ca isotopes in mice. *Anal Chim Acta*. 2020;1130:137-145. https://doi.org/10.1016/j.aca.2020.07.045
12. González de Vega C, Chernonozhkin SM, Grigoryan R, Costas-Rodríguez M, Vanhaecke F. Characterization of the new isotopic reference materials IRMM-524A and ERM-AE143 for Fe and mg isotopic analysis of geological and biological samples. *J Anal at Spectrom*. 2020;35(11):2517-2529. https://doi.org/10.1039/D0JA00225A
13. Bao Z, Zong C, Chen K, Lv N, Yuan H. Chromatographic purification of ca and mg from biological and geological samples for isotope analysis by MC-ICP-MS. *Int J Mass Spectrom*. 2020;448:116268. https://doi.org/10.1016/j.ijms.2019.116268
14. Galy A, Belshaw NS, Halicz L, O'Nions RK. High-precision measurement of magnesium isotopes by multiple- collector inductively coupled plasma mass spectrometry. *Int J Mass Spectrom*. 2001;208(1–3):89-98.
15. Galy A, Yoffe O, Janney PE, et al. Magnesium isotope heterogeneity of the isotopic standard SRM980 and new reference materials for magnesium-isotope-ratio measurements. *J Anal at Spectrom*. 2003;18(11):1352. https://doi.org/10.1039/b309273a
16. Sauzéat L, Costas-Rodríguez M, Albalat E, Mattielli N, Vanhaecke F, Balter V. Inter-comparison of stable iron, copper and zinc isotopic compositions in six reference materials of biological origin. *Talanta*. 2021;221:121576. https://doi.org/10.1016/j.talanta.2020.121576
17. Young ED, Galy A, Nagahara H. Kinetic and equilibrium mass-dependent isotope fractionation laws in nature and their geochemical and cosmochemical significance. *Geochim Cosmochim Acta*. 2002;66(6):1095-1104. https://doi.org/10.1016/S0016-7037(01)00832-8
18. Bohlin MS, Misra S, Lloyd N, Elderfield H, Bickle MJ. High-precision determination of lithium and magnesium isotopes utilising single column separation and multi-collector inductively coupled plasma mass spectrometry. *Rapid Commun Mass Spectrom*. 2018;32(2):93-104. https://doi.org/10.1002/rcm.8020
19. Craddock PR, Dauphas N. Iron isotopic compositions of geological reference materials and chondrites. *Geostand Geoanal Res*. 2011;35(1):101-123. https://doi.org/10.1111/j.1751-908X.2010.00085.x

20. Tacail T, Albalat E, Télouk P. Balter V. a simplified protocol for measurement of ca isotopes in biological samples. *J Anal at Spectrom*. 2014;29(3):529. https://doi.org/10.1039/c3ja50337b
21. Nelson F, Murase T, Kraus KA. Ion exchange procedures: I. cation exchange in concentration HCl and HClO4 solutions. *J Chromatogr a*. 1964;13:503-535. https://doi.org/10.1016/S0021-9673(01)95146-5
22. Tian H-C, Yang W, Li S-G, Ke S, Chu Z-Y. Origin of low δ26Mg basalts with EM-I component: Evidence for interaction between enriched lithosphere and carbonated asthenosphere. *Geochim Cosmochim Acta*. 2016;188:93-105. https://doi.org/10.1016/j.gca.2016.05.021
23. Shalev N, Farkaš J, Fietzke J, et al. Mg isotope Interlaboratory comparison of reference materials from earth-surface low-temperature environments. *Geostand Geoanal Res*. 2018;42(2):205-221. https://doi.org/10.1111/ggr.12208
24. Opfergelt S, Burton KW, Georg RB, et al. Magnesium retention on the soil exchange complex controlling mg isotope variations in soils, soil solutions and vegetation in volcanic soils, Iceland. *Geochim Cosmochim Acta*. 2014;125:110-130. https://doi.org/10.1016/j.gca.2013.09.036
25. Opfergelt S, Georg RB, Delvaux B, Cabidoche Y-M, Burton KW, Halliday AN. Mechanisms of magnesium isotope fractionation in volcanic soil weathering sequences, Guadeloupe. *Earth Planet Sci Lett*. 2012;341-344:176-185. https://doi.org/10.1016/j.epsl.2012.06.010
26. Liu M, Yang H, Mao Y. Magnesium and liver disease. *Ann Transl Med*. 2019;7(20):578-578. https://doi.org/10.21037/atm.2019.09.70
27. Li W, Zhu X, Song Y, et al. Intakes of magnesium, calcium and risk of fatty liver disease and prediabetes. *Public Health Nutr*. 2018;21(11):2088-2095. https://doi.org/10.1017/S1368980018000642
28. Mavromatis V, Rinder T, Prokushkin AS, et al. The effect of permafrost, vegetation, and lithology on mg and Si isotope composition of the Yenisey River and its tributaries at the end of the spring flood. *Geochim Cosmochim Acta*. 2016;191:32-46. https://doi.org/10.1016/j.gca.2016.07.003
29. Geske A, Lokier S, Dietzel M, Richter DK, Buhl D. Immenhauser a. magnesium isotope composition of sabkha porewater and related (sub-)recent stoichiometric dolomites, Abu Dhabi (UAE). *Chem Geol*. 2015;393-394:112-124. https://doi.org/10.1016/j.chemgeo.2014.11.020
30. Walter BF. Exploration of hydrothermal carbonate magnesium isotope signatures as tracers for continental fluid aquifers, Schwarzwald mining district, SW Germany. *Chem Geol*. 2015;400:87-105.
31. Lee S-W, Ryu J-S, Lee K-S. Magnesium isotope geochemistry in the Han River, South Korea. *Chem Geol*. 2014;364:9-19. https://doi.org/10.1016/j.chemgeo.2013.11.022
32. Choi MS, Ryu J-S, Lee S-W, Shin HS, Lee K-S. A revisited method for mg purification and isotope analysis using cool-plasma MC-ICP-MS. *J Anal at Spectrom*. 2012;27(11):1955. https://doi.org/10.1039/c2ja30191a
33. Wimpenny J, Burton KW, James RH, Gannoun A, Mokadem F, Gíslason SR. The behaviour of magnesium and its isotopes during glacial weathering in an ancient shield terrain in West Greenland. *Earth Planet Sci Lett*. 2011;304(1–2):260-269. https://doi.org/10.1016/j.epsl.2011.02.008
34. Immenhauser A, Buhl D, Richter D, et al. Magnesium-isotope fractionation during low-mg calcite precipitation in a limestone cave – Field study and experiments. *Geochim Cosmochim Acta*. 2010;74(15):4346-4364. https://doi.org/10.1016/j.gca.2010.05.006
35. Hippler D, Buhl D, Witbaard R, Richter DK, Immenhauser A. Towards a better understanding of magnesium-isotope ratios from marine skeletal carbonates. *Geochim Cosmochim Acta*. 2009;73(20):6134-6146. https://doi.org/10.1016/j.gca.2009.07.031
36. Wombacher F, Eisenhauer A, Heuser A, Weyer S. Separation of mg, ca and Fe from geological reference materials for stable isotope ratio analyses by MC-ICP-MS and double-spike TIMS. *J Anal at Spectrom*. 2009;24(5):627-636. https://doi.org/10.1039/B820154D
37. Pogge von Strandmann PAE, James RH, van Calsteren P, Gíslason SR, Burton KW. Lithium, magnesium and uranium isotope behaviour in the estuarine environment of basaltic islands. *Earth Planet Sci Lett*. 2008;274(3–4):462-471. https://doi.org/10.1016/j.epsl.2008.07.041
38. Pearson NJ, Griffin WL, Alard O, O'Reilly SY. The isotopic composition of magnesium in mantle olivine: Records of depletion and metasomatism. *Chem Geol*. 2006;226(3–4):115-133. https://doi.org/10.1016/j.chemgeo.2005.09.029
39. Bialik OM, Wang X, Zhao S, Waldmann ND, Frank R, Li W. Mg isotope response to dolomitization in hinterland-attached carbonate platforms: Outlook of δ26Mg as a tracer of basin restriction and seawater mg/ca ratio. *Geochim Cosmochim Acta*. 2018;235:189-207. https://doi.org/10.1016/j.gca.2018.05.024
40. Riechelmann S, Mavromatis V, Buhl D, et al. Echinoid skeletal carbonate as archive of past seawater magnesium isotope signatures – Potential and limitations. *Geochim Cosmochim Acta*. 2018;235:333-359. https://doi.org/10.1016/j.gca.2018.06.008
41. Hu Z, Hu W, Wang X, et al. Resetting of mg isotopes between calcite and dolomite during burial metamorphism: Outlook of mg isotopes as geothermometer and seawater proxy. *Geochim Cosmochim Acta*. 2017;208:24-40. https://doi.org/10.1016/j.gca.2017.03.026
42. Ryu J-S, Vigier N, Decarreau A, et al. Experimental investigation of mg isotope fractionation during mineral dissolution and clay formation. *Chem Geol*. 2016;445:135-145. https://doi.org/10.1016/j.chemgeo.2016.02.006
43. Karasinski J, Bulska E, Wojciechowski M, Halicz L, Krata AA. High precision direct analysis of magnesium isotope ratio by ion chromatography/multicollector-ICPMS using wet and dry plasma conditions. *Talanta*. 2017;165:64-68. https://doi.org/10.1016/j.talanta.2016.12.033
44. Wang Z-Z, Liu S-A, Ke S, Liu Y-C, Li S-G. Magnesium isotopic heterogeneity across the cratonic lithosphere in eastern China and its origins. *Earth Planet Sci Lett*. 2016;451:77-88. https://doi.org/10.1016/j.epsl.2016.07.021
45. Chen Y-X, Schertl H-P, Zheng Y-F, Huang F, Zhou K, Gong Y-Z. Mg–O isotopes trace the origin of mg-rich fluids in the deeply subducted continental crust of Western Alps. *Earth Planet Sci Lett*. 2016;456:157-167. https://doi.org/10.1016/j.epsl.2016.09.010
46. Ke S, Teng F-Z, Li S-G, et al. Mg, Sr, and O isotope geochemistry of syenites from Northwest Xinjiang, China: Tracing carbonate recycling during Tethyan oceanic subduction. *Chem Geol*. 2016;437:109-119. https://doi.org/10.1016/j.chemgeo.2016.05.002
47. Huang J-X, Xiang Y, An Y, et al. Magnesium and oxygen isotopes in Roberts victor eclogites. *Chem Geol*. 2016;438:73-83. https://doi.org/10.1016/j.chemgeo.2016.05.030
48. An Y, Wu F, Xiang Y, et al. High-precision mg isotope analyses of low-mg rocks by MC-ICP-MS. *Chem Geol*. 2014;390:9-21. https://doi.org/10.1016/j.chemgeo.2014.09.014
49. Teng F-Z, Yin Q-Z, Ullmann CV, et al. Interlaboratory comparison of magnesium isotopic compositions of 12 felsic to ultramafic igneous rock standards analyzed by MC-ICPMS. *Geochem Geophys Geosyst*. 2015;16(9):3197-3209. https://doi.org/10.1002/2015GC005939
50. Shen B, Wimpenny J, Lee CTA, Tollstrup D, Yin Q-Z. Magnesium isotope systematics of endoskarns: Implications for wallrock reaction in magma chambers. *Chem Geol*. 2013;356:209-214. https://doi.org/10.1016/j.chemgeo.2013.08.018
51. Huang K-J, Teng F-Z, Wei G-J, Ma J-L, Bao Z-Y. Adsorption- and desorption-controlled magnesium isotope fractionation during extreme weathering of basalt in Hainan Island, China. *Earth Planet Sci Lett*. 2012;359–360:73-83. https://doi.org/10.1016/j.epsl.2012.10.007
52. Pogge von Strandmann PAE, Elliott T, Marschall HR, et al. Variations of Li and mg isotope ratios in bulk chondrites and mantle xenoliths.

Geochim Cosmochim Acta. 2011;75(18):5247-5268. https://doi.org/10.1016/j.gca.2011.06.026
53. Hoang THA, Choi SH, Yu Y, Pham TH, Nguyen KH, Ryu J-S. Geochemical constraints on the spatial distribution of recycled oceanic crust in the mantle source of late Cenozoic basalts, Vietnam. *Lithos*. 2018;296-299:382-395. https://doi.org/10.1016/j.lithos.2017.11.020
54. Wang X-J, Chen L-H, Hofmann AW, et al. Mantle transition zone-derived EM1 component beneath NE China: Geochemical evidence from Cenozoic potassic basalts. *Earth Planet Sci Lett*. 2017;465:16-28. https://doi.org/10.1016/j.epsl.2017.02.028
55. Zhong Y, Chen L-H, Wang X-J, Zhang G-L, Xie L-W, Zeng G. Magnesium isotopic variation of oceanic island basalts generated by partial melting and crustal recycling. *Earth Planet Sci Lett*. 2017;463:127-135. https://doi.org/10.1016/j.epsl.2017.01.040
56. Tian H-C, Yang W, Li S-G, Ke S. Could sedimentary carbonates be recycled into the lower mantle? Constraints from mg isotopic composition of Emeishan basalts. *Lithos*. 2017;292-293:250-261. https://doi.org/10.1016/j.lithos.2017.09.007
57. Chapela Lara M, Buss HL, Pogge von Strandmann PAE, Schuessler JA, Moore OW. The influence of critical zone processes on the mg isotope budget in a tropical, highly weathered andesitic catchment. *Geochim Cosmochim Acta*. 2017;202:77-100. https://doi.org/10.1016/j.gca.2016.12.032
58. zCheng Z, Zhang Z, Hou T, et al. Decoupling of mg–C and Sr–Nd–O isotopes traces the role of recycled carbon in magnesiocarbonatites from the Tarim large Igneous Province. *Geochim Cosmochim Acta*. 2017;202:159-178. https://doi.org/10.1016/j.gca.2016.12.036
59. Maher K, Johnson N-C, Jackson A, et al. A spatially resolved surface kinetic model for forsterite dissolution. *Geochim Cosmochim Acta*. 2016;174:313-334. https://doi.org/10.1016/j.gca.2015.11.019
60. Hu Y, Teng F-Z, Zhang H-F, Xiao Y, Su B-X. Metasomatism-induced mantle magnesium isotopic heterogeneity: Evidence from pyroxenites. *Geochim Cosmochim Acta*. 2016;185:88-111. https://doi.org/10.1016/j.gca.2015.11.001
61. Cheng Z, Zhang Z, Hou T, Santosh M, Zhang D, Ke S. Petrogenesis of nephelinites from the Tarim large Igneous Province, NW China: Implications for mantle source characteristics and plume–lithosphere interaction. *Lithos*. 2015;220-223:164-178. https://doi.org/10.1016/j.lithos.2015.02.002
62. Liu X-M, Teng F-Z, Rudnick R-L, McDonough W-F, Cummings ML. Massive magnesium depletion and isotope fractionation in weathered basalts. *Geochim Cosmochim Acta*. 2014;135:336-349. https://doi.org/10.1016/j.gca.2014.03.028
63. Teng F-Z, Li W-Y, Ke S, et al. Magnesium isotopic compositions of international geological reference materials. *Geostand Geoanal Res*. 2015;39(3):329-339. https://doi.org/10.1111/j.1751-908X.2014.00326.x
64. Chopra R, Richter F-M, Bruce Watson E, Scullard C-R. Magnesium isotope fractionation by chemical diffusion in natural settings and in laboratory analogues. *Geochim Cosmochim Acta*. 2012;88:1-18. https://doi.org/10.1016/j.gca.2012.03.039
65. Huang F, Zhang Z, Lundstrom CC, Zhi X. Iron and magnesium isotopic compositions of peridotite xenoliths from eastern China. *Geochim Cosmochim Acta*. 2011;75(12):3318-3334. https://doi.org/10.1016/j.gca.2011.03.036
66. Huang F, Glessner J, Ianno A, Lundstrom C, Zhang Z. Magnesium isotopic composition of igneous rock standards measured by MC-ICP-MS. *Chem Geol*. 2009;268(1–2):15-23. https://doi.org/10.1016/j.chemgeo.2009.07.003
67. Fan B, Zhao Z-Q, Tao F, et al. The geochemical behavior of mg isotopes in the Huanghe basin, China. *Chem Geol*. 2016;426:19-27. https://doi.org/10.1016/j.chemgeo.2016.01.005
68. Bourdon B, Tipper ET, Fitoussi C, Stracke A. Chondritic mg isotope composition of the earth. *Geochim Cosmochim Acta*. 2010;74(17):5069-5083. https://doi.org/10.1016/j.gca.2010.06.008
69. Teng F-Z, Wadhwa M, Helz RT. Investigation of magnesium isotope fractionation during basalt differentiation: Implications for a chondritic composition of the terrestrial mantle. *Earth Planet Sci Lett*. 2007;261(1–2):84-92. https://doi.org/10.1016/j.epsl.2007.06.004

SUPPORTING INFORMATION

Additional supporting information may be found online in the Supporting Information section at the end of this article.

How to cite this article: Le Goff S, Albalat E, Dosseto A, Godin J-P, Balter V. Determination of magnesium isotopic ratios of biological reference materials via multi-collector inductively coupled plasma mass spectrometry. *Rapid Commun Mass Spectrom*. 2021;35:e9074. https://doi.org/10.1002/rcm.9074